Journal of Chromatography B, 1000 (2015) 14–21

Contents lists available at ScienceDirect

Journal of Chromatography B

journal homepage: www.elsevier.com/locate/chromb

Lipidomic differentiation between human kidney tumors and surrounding normal tissues using HILIC-HPLC/ESI–MS and multivariate data analysis

Eva Cífková[a], Michal Holčapek[a,*], Miroslav Lísa[a], David Vrána[b], Bohuslav Melichar[b], Vladimír Študent[c]

[a] University of Pardubice, Faculty of Chemical Technology, Department of Analytical Chemistry, Studentská 573, 532 10 Pardubice, Czech Republic
[b] Palacký University, Medical School and Teaching Hospital, Department of Oncology, I.P. Pavlova 6, 775 20 Olomouc, Czech Republic
[c] Palacký University, Faculty of Medicine and Dentistry, Department of Urology, I.P. Pavlova 6, 775 20 Olomouc, Czech Republic

ARTICLE INFO

Article history:
Received 27 January 2015
Received in revised form 24 March 2015
Accepted 5 July 2015
Available online 13 July 2015

Keywords:
Lipidomics
Kidney cancer
Glycerophospholipids
HILIC-HPLC/ESI–MS
Multivariate data analysis

ABSTRACT

The characterization of differences among polar lipid classes in tumors and surrounding normal tissues of 20 kidney cancer patients is performed by hydrophilic interaction liquid chromatography (HILIC) coupled to electrospray ionization mass spectrometry (ESI–MS). The detailed analysis of identified lipid classes using relative abundances of characteristic ions in negative- and positive-ion modes is used for the determination of more than 120 individual lipid species containing attached fatty acyls of different chain length and double bond number. Lipid species are described using relative abundances, providing a better visualization of lipidomic differences between tumor and normal tissues. The multivariate data analysis methods using unsupervised principal component analysis (PCA) and supervised orthogonal partial least square (OPLS) are used for the characterization of statistically significant differences in identified lipid species. Ten most significant up- and down-regulated lipids in OPLS score plots are also displayed by box plots. A notable increase of relative abundances of lipids containing four and more double bonds is detected in tumor compared to normal tissues.

1. Introduction

Kidney cancer ranks among 10 most common cancers for both men and women, representing approximately 3% of adult tumors [1,2]. Renal cell cancer (RCC) represents more than 90% of malignant kidney tumors. The principal histological RCC subtypes include clear cell RCC (70–80%), papillary RCC (10–15%) and chromophobe RCC (3–5%). RCC is characterized by the resistance to virtually all cytotoxic agents. Before the advent of targeted therapy, surgery was the only effective treatment of this tumor. However, only a small proportion of patients with metastatic disease could be cured with surgery. Cytokines, the only systemic agents with some reproducible activity, were effective only in a minority of patients. Targeted therapy has changed the natural course of metastatic RCC. In the last decade, a number of targeted agents have been introduced, including multiple tyrosine kinase inhibitors sunitinib, sorafenib, axitinib and pazopanib, the monoclonal antibody bevacizumab and mammalian target of rapamycin inhibitors everolimus and temsirolimus. Despite this progress, few, if any, patients are cured by currently available drugs. In the search of new effective therapies novel molecular targets associated with malignant transformation have to be identified.

Lipids play an essential role in many biological processes, including the formation of cellular or intracellular membranes and compartments, the energy storage, the synthesis of hormones and the signal transduction [2–4]. The disruption of lipid metabolism and associated signaling pathways alters cellular function resulting in a spectrum of disorders, including the cancer. For example, palmitic acid (16:0) is a substrate for the formation of lipids required for the cellular proliferation and tumorigenic

Abbreviations: aCN, average carbon number; aDB, average double bond; CE, cholesteryl esters; CN, carbon number; DB, double bond; ESI, electrospray ionization; HILIC, hydrophilic interaction liquid chromatography; HPLC, high-performance liquid chromatography; Chol, cholesterol; IS, internal standard; LPA, lysophosphatidic acids; LPC, lysophosphatidylcholines; MDA, multivariate data analysis; MS, mass spectrometry; NP, normal phase; OPLS, orthogonal partial least square; PC, phosphatidylcholines; PCA, principal component analysis; PE, phosphatidylethanolamines; PI, phosphatidylinositols; RCC, renal cell cancer; RF, response factor; RP, reversed phase; SM, sphingomyelins; TG, triacylglycerol.

* Corresponding author. Fax: +420 466037068.
E-mail address: Michal.Holcapek@upce.cz (M. Holčapek).

http://dx.doi.org/10.1016/j.jchromb.2015.07.011
1570-0232/

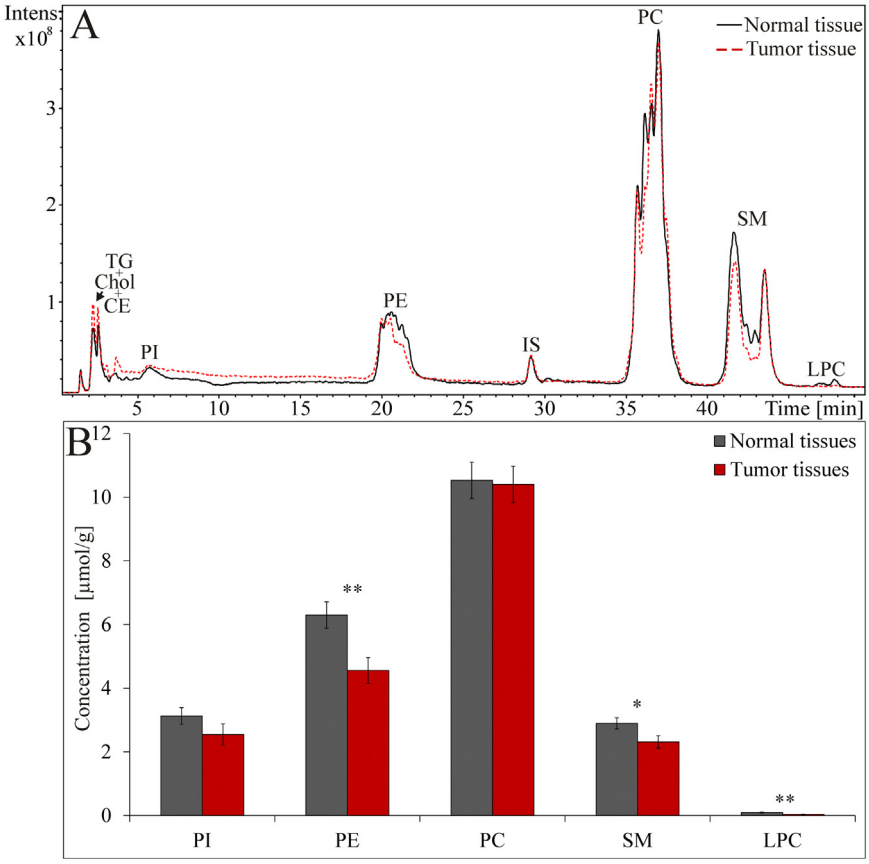

Fig. 1. (A) Positive-ion HILIC-HPLC/ESI–MS of total lipid extracts of normal (black line) and tumor (red line) tissues of a patient with clear cell type of kidney cancer. HPLC conditions: column Spherisorb Si (250 × 4.6 mm, 5 μm), flow rate 1 mL/min, separation temperature 40 °C, gradient 0 min – 94% A + 6% B, 60 min – 77% A + 23% B, where A is acetonitrile and B is 5 mM aqueous ammonium acetate. (B) Comparison of average concentrations [μmol/g] of individual lipid classes in normal and tumor tissues for 20 patients with their standard errors. Peak annotation: TG – triacylglycerols, Chol – cholesterol, CE – cholesteryl esters, PI – phosphatidylinositols, PE – phosphatidylethanolamines, IS – internal standard, PC – phosphatidylcholines, SM – sphingomyelins, LPC – lysophosphatidylcholines. Statistically significant differences according to *T*-test are indicated by an asterisk, where * refers to the significance $p \leq 0.05$ and ** $p \leq 0.01$. (For interpretation of the references to color in this figure legend, the reader is referred to the web version of this article.)

lipid signaling, while lysophosphatidic acids (LPA) and some specific eicosanoids serve as proliferative receptors. On the other hand, ceramides and sphingosines have antiproliferative and proapoptotic activity and are involved in the programed cell death [3–7]. Furthermore, arachidonic acid (20:4) belongs to major *n*-6 polyunsaturated fatty acids that affect increased production of inflammatory mediators [4].

Many studies addressing the lipidomic analysis of various biological samples benefit from high sensitivity and selectivity of the coupling of high-performance liquid chromatography and mass spectrometry (HPLC/MS). The separation in normal phase (NP) [8,9] or hydrophilic interaction liquid chromatography (HILIC) systems [10] enables the lipid class separation according to the polarity. Reversed phase (RP) HPLC on nonpolar stationary phases is frequently used for the separation of individual lipid species according to the fatty acyl chain length [11]. The quantitative analysis of lipids can be performed using the MS with the direct infusion (shotgun lipidomics) or HPLC/MS approaches. Shotgun is the most frequently used technique due to the rapid nontargeted analysis using precursor ion and neutral loss scans, which are well characterized for many lipid classes [12–14]. HPLC/MS approach was developed for the quantitation of separated lipid classes using the internal standard (IS) per each lipid class [15] or the combination of the single IS and response factors (RF) of individual lipid classes related with this IS [16,17].

Lipidomic analysis of RCC tissues and normal kidney tissues was performed using HPLC/MS [18], where significantly increased levels of cholesteryl esters (CE) and triacylglycerols (TG) and decreased levels of phosphatidylethanolamines (PE) and sphingomyelins (SM) in tumor tissues were reported. Mass spectrometry imaging using matrix-assisted laser desorption/ionization or desorption electrospray ionization was used for the relative comparison of tumor and surrounding normal tissues [19–22]. Increased absolute intensities for PI 18:0/20:4, PS 18:0/18:1 and PI 22:4/18:0 were reported [19,21] in kidney tumor tissues using the desorption electrospray ionization imaging. Analyses of lipids in plasma from RCC patients using ^{31}P nuclear magnetic resonance showed decreased concentrations of lysophosphatidylcholines (LPC) in comparison with healthy volunteers [23].

Multivariate data analysis (MDA) is a valuable approach for the evaluation of extensive data sets, providing significantly more information compared to the univariate data analysis [24–27]. The principal component analysis (PCA) is the most widespread nonsupervised method for the visualization of data sets using converted uncorrelated variables called principal components. Score plots serve for the projection of clustering of observed data, while loading plots describe clustering patterns. Orthogonal partial least square (OPLS) is a supervised method, where the group identification is set up in model parameters. OPLS method may use S-plots for a better visualization of clustering patterns including the influence of magnitude and reliability of variables.

The aim of the present study is to characterize lipidomic differences between kidney tumors and surrounding normal tissues in a cohort of 20 kidney cancer patients using our validated HILIC-

HPLC/ESI–MS method [17]. This method allows the quantitation of five lipid classes separated in HILIC mode and also the detailed analysis of individual lipid species inside these classes using relative abundances of characteristic ions in the negative- and positive-ion ESI mass spectra. The statistical evaluation of obtained data set for all patients using unsupervised PCA and supervised OPLS enables to identification of lipids with the highest impact on the group separation.

2. Experimental

2.1. Materials

Acetonitrile, methanol, 2-propanol (all HPLC/MS grade), chloroform (HPLC grade stabilized by 0.5-1% ethanol), ammonium acetate and sodium chloride were purchased from Sigma–Aldrich (St. Louis, MO, USA). Deionized water was prepared with a Demiwa 5-roi purification system (Watek, Ledeč nad Sázavou, Czech Republic). *N*-dodecanoyl-heptadecasphing-4-enine-1-phosphoethanolamine (d17:1/12:0) used as an internal standard (IS) for the quantitative analysis was purchased from Avanti Polar Lipids (Alabaster, AL, USA). Tumor tissues and surrounding normal tissues of 20 kidney cancer patients (Table S1) were obtained from the Department of Urology, Palacký University, Faculty of Medicine and Dentistry and University Hospital, Olomouc, Czech Republic. The study was approved by the Hospital Ethical Committee, and all patients signed informed consent.

2.2. Sample preparation

Samples of kidney tumor and normal kidney tissue were obtained during the surgery, immediately frozen and stored at −80 °C until the sample processing and the analysis. Human kidney tissues were prepared using chloroform–methanol–water extraction according to a Folch method [28]. Briefly, 250 mg of kidney tissue and 25 μL of 3.3 mg/mL IS were homogenized with 5 mL of chloroform–methanol (2:1, v/v) mixture. The filtered homogenate was mixed with 1 mL of 1 mol/L sodium chloride and centrifuged at 3000 rpm for 5 min at room temperature. Bottom chloroform layer containing lipids was evaporated by a stream of nitrogen and redissolved in 1 mL of chloroform–2-propanol mixture (1:1, v/v).

2.3. HPLC/MS conditions

Total lipid extracts were analyzed by HPLC/MS method described previously [10,17]. The liquid chromatograph Agilent 1290 series (Agilent Technologies, Waldbronn, Germany) was coupled with the Esquire 3000 ion trap analyzer (Bruker Daltonics, Bremen, Germany). The separation of individual lipid classes was performed on a Spherisorb Si column (250 × 4.6 mm, 5 μm, Waters, Milford, MA, USA), a flow rate of 1 mL/min, an injection volume of 1 μL, column temperature of 40 °C and a mobile phase gradient: 0 min – 94% A + 6% B, 60 min – 77% A + 23% B, where A was acetonitrile and B was 5 mmol/L aqueous ammonium acetate. Lipids were detected in positive- and negative-ion ESI–MS modes in the mass range m/z 50–1000 with the setting of pressure of the nebulizing gas 60 psi, drying gas flow rate 10 L/min and temperature of the drying gas 365 °C. The quantitation of individual lipid classes was achieved by the single IS and response factors obtained from calibration curves as described previously [17]. Individual lipid species were analyzed using relative abundances of deprotonated molecules $[M\text{-}H]^-$ for PE and PI classes and $[M\text{-}CH_3]^-$ ions for PC class in the negative-ion mode [17]. Individual SM species were analyzed using relative abundances of protonated molecules $[M+H]^+$ in the positive-ion mode due to the low signal intensity in the negative-ion mode. The low energy collision induced dissociation tandem mass spectrometry (MS/MS) experiments were performed for the most significant lipid species with the isolation width of *m/z* 4, the collision amplitude of 1 V and helium as a collision gas.

2.4. Statistical data analysis

MDA was performed using PCA and OPLS methods in the SIMCA software, version 13.0 (Umetrics, Umeå, Sweden). Data were preprocessed before the statistical analysis using the Pareto scaling. All models were characterized by score plots, loading plots and S-plots listed in Table S2. Statistically significant differences in graphs were calculated using the *T*-test, where * refers to the significance $p \leq 0.05$ (5%), ** $p \leq 0.01$ (1%) and *** $p \leq 0.01$ (0.1%). Box plots describe values of median, minimum, maximum and the variability of data sets using the first and third quartiles.

3. Results and discussion

3.1. Quantitative analysis of polar lipid classes

Among 20 samples analyzed, 19 cases are RCC (18 cases of clear cell RCC and one case of papillary RCC), while the rare Wilms tumor is diagnosed in one case. No statistically relevant differences are observed in our data for clear cell RCC, papillary RCC and Wilms tumor, so the data are treated as one group of kidney cancer. Total lipid extracts are analyzed using our previously developed HILIC-HPLC/ESI–MS method [17,29], which was validated for the quantitation of polar lipid classes using single IS (sphingosyl PE d17:1/12:0) and response factors calculated from their calibration curves [16,17]. Fig. 1A shows a baseline separation of PI, PE, PC, SM and LPC classes and the IS. Different peak shapes of some lipid classes are observed between normal (gray line) and tumor (red line) tissues for one patient, which is caused by different lipidomic composition inside these classes (Table S3). The present HILIC-HPLC/ESI–MS method is not applicable for the quantitation of nonpolar lipid classes, namely TG, CE and cholesterol (Chol), due to their elution in the system void volume. Mean lipid class concentrations of 20 kidney cancer patients significantly differ between normal (gray columns) and tumor (red columns) tissues for some lipid classes, with PE, LPC and SM showing the highest variance (Fig. 1B). Numerical values of mean concentrations and their standard deviations are listed in Table S4. Decreased levels of PE, SM and LPC in kidney tumor tissues in comparison with surrounding normal tissues are in agreement with previous reports [18,23].

3.2. Detailed analysis of individual lipid species

Individual lipid species inside classes are described using relative abundances of characteristic ions in ESI mass spectra obtained by the peak integration of given lipid class in the HILIC chromatogram. Deprotonated molecules $[M\text{-}H]^-$ are used for the analysis of individual PE and PI species and $[M\text{-}CH_3]^-$ ions for PC in the negative-ion mode, while protonated molecules $[M+H]^+$ are used for SM species in the positive-ion mode. In this study, the relative quantitation (in%) calculated based on relative abundances of their characteristic ions is preferred for individual lipid species (Figs. 2 and 3,), which is especially useful for better visualization of lipid changes between tumor and normal tissues. The absolute quantitative data (in μmol/g) are calculated as relative abundances of individual lipid species multiplied by the total concentration of this lipid class (Fig. S1 and S2). The deisotoping of mass spectra for all described lipid species is performed using the Excel script, where isotopic patterns are calculated using the Isotope pattern software (Bruker Daltonics). The identification of prevalent combination of

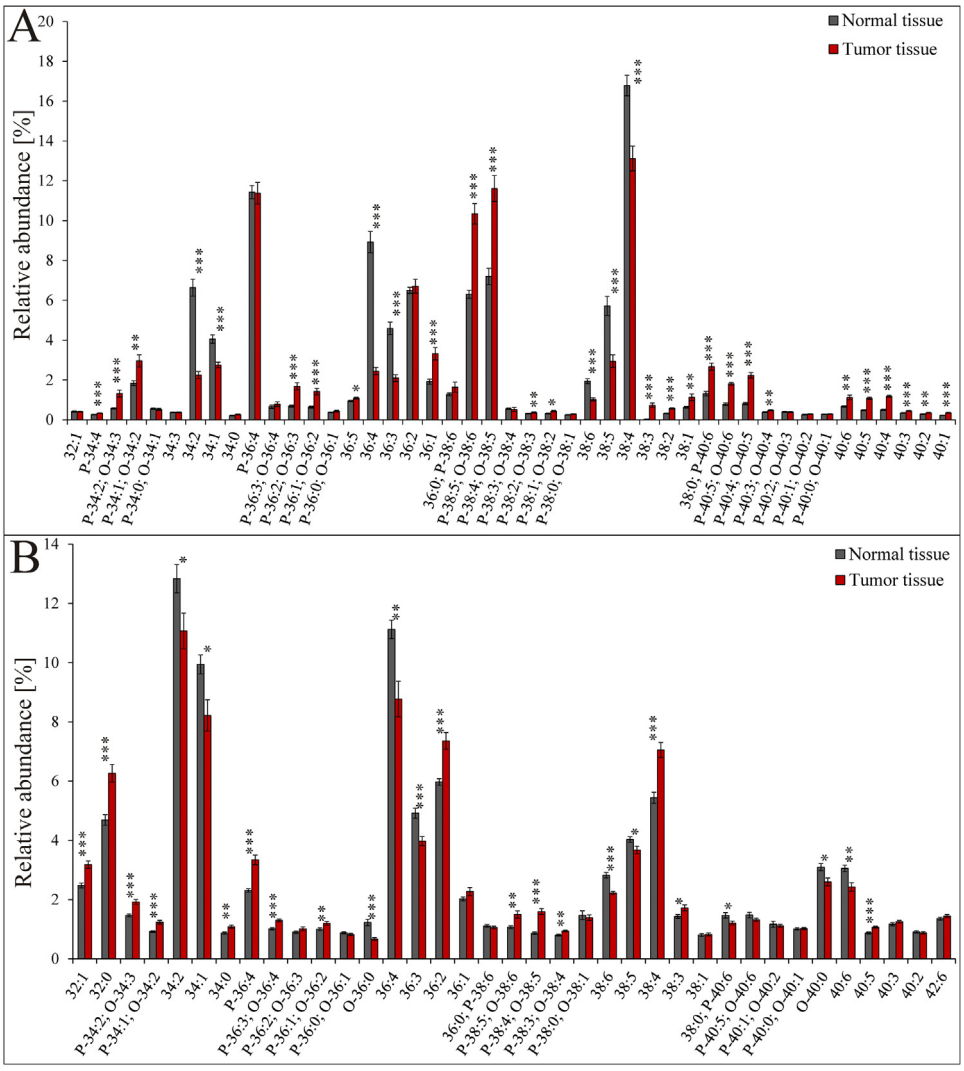

Fig. 2. Relative abundances [%] of individual species in normal and tumor tissues of 20 patients with kidney cancer: (A) PE and (B) PC determined by relative abundances of $[M\text{-}H]^-$ and $[M\text{-}CH_3]^-$ ions, respectively, in the negative-ion HILIC-HPLC/ESI–MS. Statistically significant differences according to *T*-test are indicated by an asterisk, where * refers to the significance $p \leq 0.05$, ** $p \leq 0.01$, and *** $p \leq 0.001$.

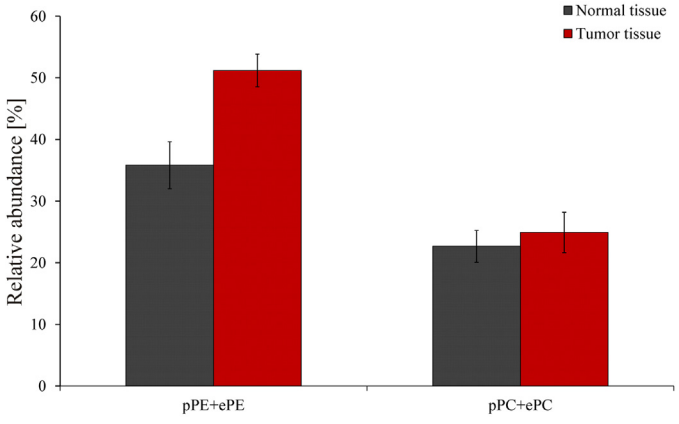

Fig. 3. Comparison of relative abundances of the sum of pPE+ePE species and the sum of pPC+ePC species in normal and tumor tissues for 20 patients. Bars indicate standard error.

attached fatty acyls and their positions on the glycerol skeleton of the most significant lipid species for differentiation of tumor and normal tissues was additionally performed using MS/MS spectra in the negative-ion mode. Individual lipid species are characterized by attached fatty acyls annotated by their total carbon number and double bond number (CN:DB). Some lipid species (e.g., PE and PC) can also differ in the type of fatty acyl linkage to the glycerol skeleton in the *sn*-1 position. The ester linkage of fatty acyls in both *sn*-1 and *sn*-2 positions (diacyls) is referred as aPE and aPC. The ether linkage of fatty acyls in *sn*-1 position (1-alkyl-2-acyl) is referred as ethers (ePE and ePC) and the vinyl ether linkage in *sn*-1 position (1-alkenyl-2-acyl) corresponds to plasmalogens (pPE and pPC).

3.3. Characterization of lipid species differences

Fig. 2A shows mean relative abundances of 45 PE species in tumor tissues (red columns) and surrounding normal tissues (gray columns) of 20 kidney cancer patients. The statistical significance is calculated using *T*-test. PE P-38:4 or O-38:5 (PE P-18:0/20:4 – prevalent combination of attached fatty acyls identified using MS/MS spectrum), PE P-38:5 or O-38:6 (PE P-18:0/20:5) and PE 36:1 (PE 18:0/18:1) are the most up-regulated PE species in tumor tissues, while PE 38:4 (PE 18:0/20:4), PE 36:4 (PE 16:0/20:4) and PE 34:2 (PE 16:0/18:2) are the most down-regulated species (Fig. 2A). All plasmalogen PE species containing more than 4 DB, which means one polyunsaturated fatty acyl on the glycerol skeleton, are up-regulated. Furthermore, the same trend is observed for PE

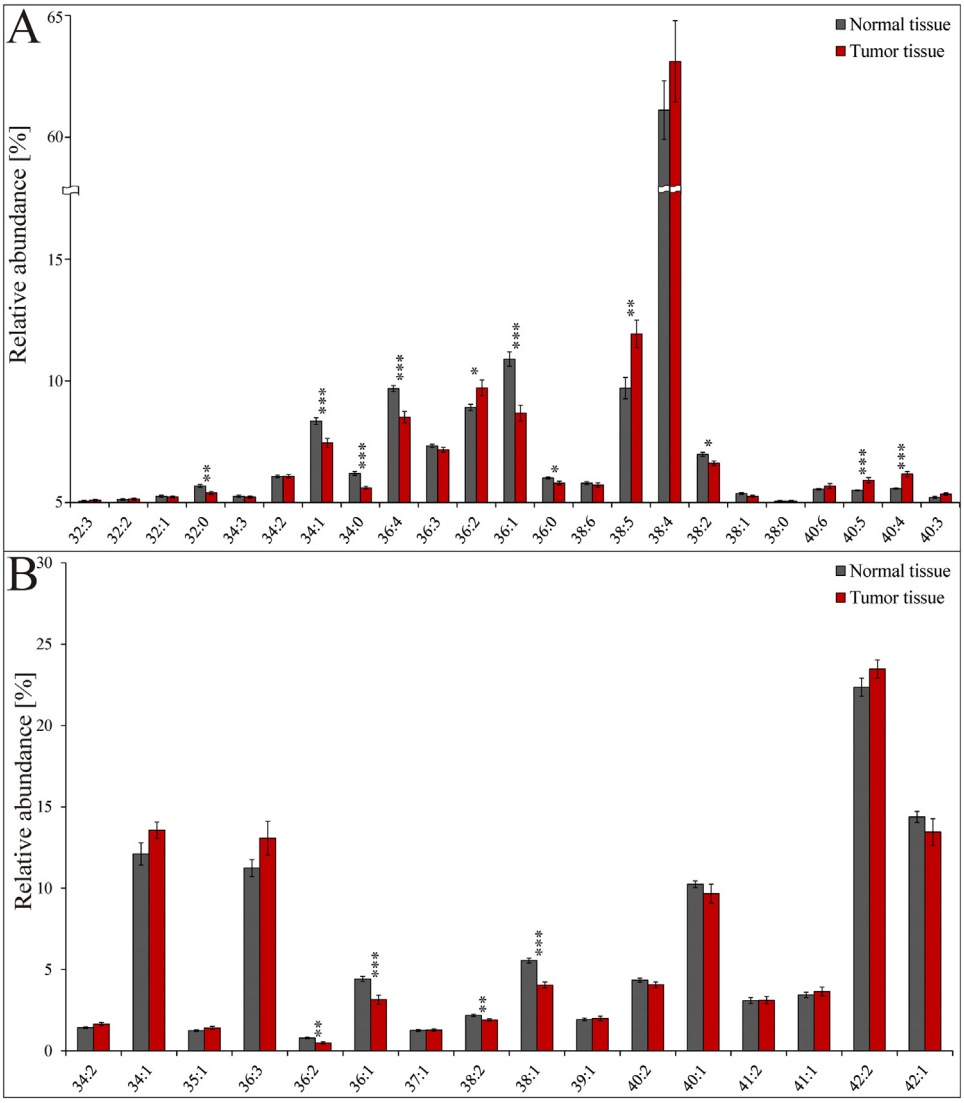

Fig. 4. Relative abundances [%] of individual species in normal and tumor tissues of 20 patients with kidney cancer: (A) PI and (B) SM determined using relative abundances of $[M-H]^-$ and $[M+H]^+$ ions, respectively, in the negative and positive-ion HILIC-HPLC/ESI–MS. Statistically significant differences according to *T*-test are indicated by an asterisk, where * refers to the significance $p \leq 0.05$, ** $p \leq 0.01$, and *** $p \leq 0.001$.

species with CN equal to 40. Relative abundances of saturated (0 DB), low unsaturated (1–3 DB) and high unsaturated (4–6 DB) fatty acyls, average CN (aCN) and average DB (aDB) are calculated in Table S3. The highest differences are observed for the group of aPE, where saturated fatty acyls decrease and high unsaturated acyls increase in tumor tissues. In other cases, differences are less pronounced.

The comparison of relative abundances of individual PC species (Fig. 2B) in tumor and normal tissues for 20 patients indicates 25 statistically significant differences in PC according to the *T*-test. The most up-regulated species are PC 38:4 (PC 18:0/20:4), PC 36:2 (PC 18:0/18:2) and PC 32:0 (PC 16:0/16:0), and down-regulated PC 34:2 (16:0/18:2), PC 36:4 (16:0/20:4) and PC 34:1 (16:0/18:1), which is in an excellent agreement with previous work [22]. Values of aCN and aDB for all PC species are similar, but significant differences between both tissues are observed for saturated and high unsaturated fatty acyls in pPC + ePC and aPC groups (Table S3). Relative abundance of saturated fatty acyls in pPC + ePC decrease about 22% in tumor tissues in comparison with surrounding normal tissues. The vinyl-ether bonds of plasmalogens are more sensitive to the oxidation by free radicals and protect membrane lipids against the oxidation associated with inflammatory response. Therefore, relative abundances of plasmalogens and ethers in PE and PC classes are reported for normal and tumor tissues in Fig. 3. The relative proportion of pPE + ePE group in PE lipid class forms 36% in normal tissues and 51% in tumor tissues, while pPC + ePC represents about 23% of all PC species in both tissues.

Relative abundances of 23 individual PI species are shown in Fig. 4A and indicate 5 statistically significant up-regulated PI species in tumor tissues, namely PI 38:5 (PI 16:0/22:5), PI 36:2 (PI 18:1/18:1), PI 40:5 (PI 18:0/22:5), PI 40:4 (PI 20:0/20:4) and PI 36:0 (18:0/18:0). These results are again in agreement with previous reports [19,21]. The species exhibiting highest down-regulated PI species are PI 36:1 (PI 18:0/18:1), PI 36:4 (PI 16:0/20:4) and PI 34:1 (PI 16:0/18:1). In comparison with other classes, the highest differences in the saturation of fatty acyls between normal and tumor tissues are observed for unsaturated fatty acyls, where low unsaturated decrease and high unsaturated increase in tumor tissues (Table S3).

Only 4 statistically significant SM species, namely SM 36:2, SM 36:1, SM 38:2 and SM 38:1, are identified using *T*-test by comparison of relative abundances of normal and tumor tissues (Fig. 4B). All

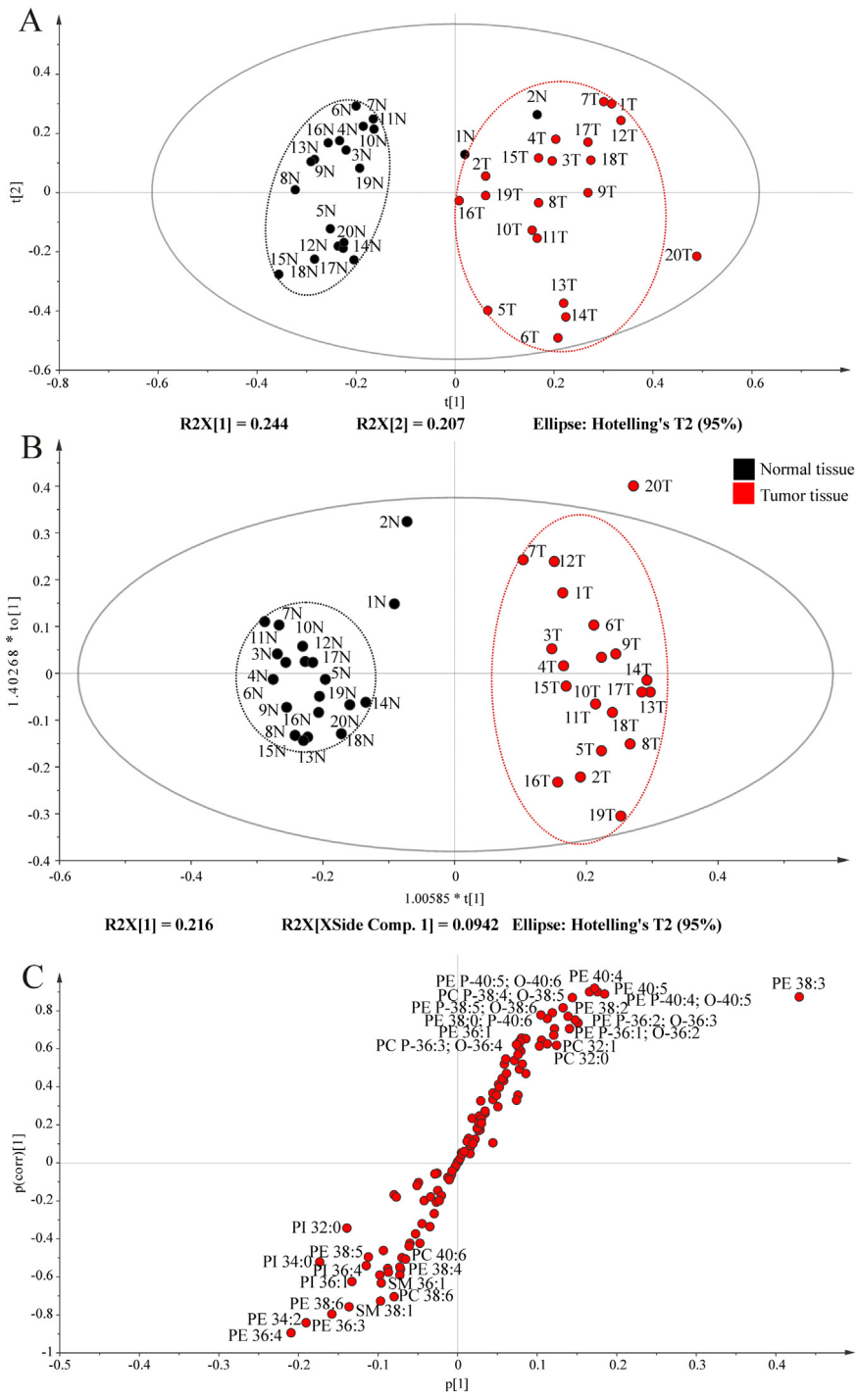

Fig. 5. Multivariate data analysis of relative abundances of all lipids in normal and tumor tissues: (A) the score plot of unsupervised PCA method, (B) the score plot and (C) the S-plot of supervised OPLS method describing up-regulated and down-regulated lipids in tumor tissues. (For interpretation of the references to color in the text, the reader is referred to the web version of this article.)

above mentioned SM species are down-regulated in tumor tissues and are formed by low unsaturated fatty acyls (Table S3). Individual fatty acyls on the glycerol skeleton cannot be identified using MS/MS spectra due to low signal intensities in the negative-ion mode. The analysis of individual LPC species cannot be performed due to low intensities of protonated molecules $[M+H]^+$ in the positive-ion ESI spectra.

HILIC-HPLC/ESI–MS method has already been used for the determination of lipidomic differences between tumor and surrounding normal tissues of 10 breast cancer patients [29]. A statistically significant increase of concentrations of all mentioned lipid classes and a decrease of relative abundances of pPE + ePE group were detected in breast tumor tissues. Lipids with the general formula 34:1 (combination of 16:0 and 18:1) are significantly increased in breast tumor tissues. Opposing trends are observed in kidney cancer. Nevertheless, glycerophospholipids with the general formula 36:4 (combination of 16:0 and 20:4) have shown marked decrease in tumor tissues for both cancer patient groups.

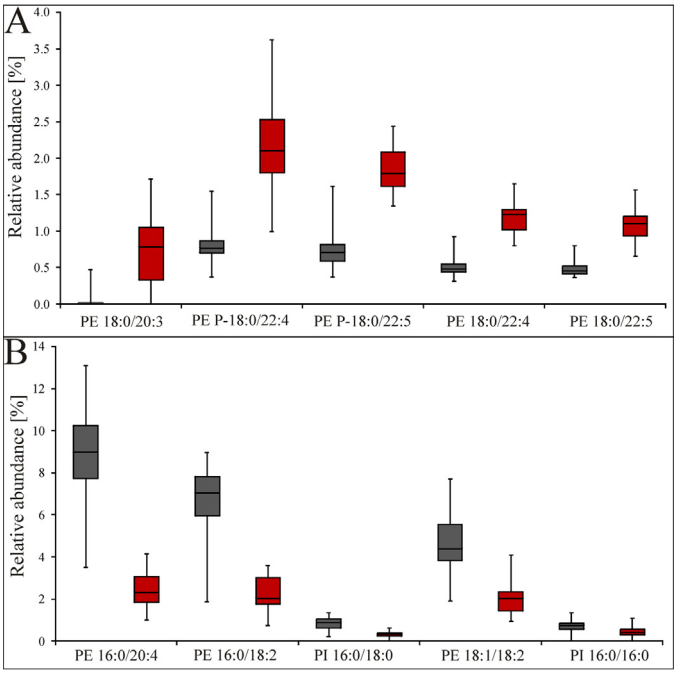

Fig. 6. Box plots describing the five most important (A) up-regulated and (B) down-regulated lipids in normal (gray) and tumor (red) tissues obtained using OPLS method. Each boxplot characterizes the variability of data sets using average values of median, first and third quartiles, minimum and maximum.

3.4. Statistical evaluation of identified lipid species

Relative abundances of all identified lipid species in normal and tumor tissues are statistically evaluated using the SIMCA software. At first, the data set is analyzed using unsupervised PCA method, which reduces the multidimensionality of the data to two-dimensional system characterized by principal components without any input specification of groups. The score plot of PCA method (Fig. 5A) shows a clear clustering of tumor tissues (red points) and normal tissues (gray points) except for 1N and 2N. The first component in PCA method explains 24.4% of the variation and the second component 20.7%. Subsequently, the supervised OPLS method is used to further improve the group clustering, because this statistical method has the input information on the group assignment. The score plot of OPLS method (Fig. 5B) shows the excellent group separation of normal and tumor tissues for all patients without any outliers. Larger variability is observed for the tumor group in contrast to the normal group, which can be probably explained by different tumor subtypes and tumor cell heterogeneity. Patterns of group clustering in OPLS score plot are visualized in the S-plot (Fig. 5C). The S-plot does not describe only the direction of regulation but also the reliability and magnitude of individual lipid species. The upper right corner of the S-plot shows up-regulated lipid species in tumor tissues, while the lower left corner down-regulated species. PE 38:3 is the up-regulated lipid with the highest reliability and high magnitude, while PE 36:4 is the most significant down-regulated lipid. Lipid species in the middle of the diagram close to zero on both axes have a low statistical significance for the group differentiation and therefore they are not annotated. The S-plot allows for the characterization of five most significant up-regulated species: PE 38:3 (PE 18:0/20:3), PE P-40:4 or O-40:5 (PE P-18:0/22:4), PE P-40:5 or O-40:6 (PE P-18:0/22:5), PE 40:4 (PE 18:0/22:4) and PE 40:5 (PE 18:0/22:5) and down-regulated: PE 36:4 (PE 16:0/20:4), PE 34:2 (16:0/18:2), PI 34:0 (16:0/18:0), PE 36:3 (PE 18:1/18:2) and PI 32:0 (PI 16:0/16:0) lipid species. These 10 lipids shown in box plots (Fig. 6) represent the largest differences between normal and tumor tissues with a low standard deviation of values. The central line in the box plot shows the value of median, the lower part represents the first quartile and the upper part is the third quartile. Extreme lines show minimum and maximum values.

Kidney cancer is a very heterogeneous group of malignant neoplasms. Most specimens examined in the present pilot study are clear cell RCC. With only a single case each of papillary RCC and Wilms tumor, no conclusions can be drawn about the lipid composition of these relatively rare kidney cancers. While currently the targeted treatment of advanced RCC relies on agents inhibiting the vascular endothelial growth factor and mammalian target of rapamycin pathways, novel drugs with other mechanisms of action start to emerge. With the advent of phosphatidylinositol 3 kinase inhibitors or other drugs targeting lipid-associated pathways, the understanding of changes of lipid metabolism in tumors may be of significance for the targeted therapy. Advances of targeted therapy are dependent on the development of predictive molecular biomarkers that may also include lipids. Present data open the way for the further research on the changes of lipid composition as biomarkers of response. The identification of lipid biomarkers could also aid in the early diagnosis, including the screening. The incidence of RCC in the Czech Republic is highest in the world, and depending on the availability of reliable diagnostic biomarkers screening programs can be envisaged.

4. Conclusions

HILIC-HPLC/ESI–MS method allows for the lipidomic characterization of tumors and surrounding normal tissues in a pilot study of 20 renal cell cancer patients. The decrease of total concentrations of PE, SM and LPC classes in tumor tissues compared to normal tissues is statistically significant according to the *T*-test. The most pronounced trend is observed for glycerophospholipids with a general formula 36:4 (PE 16:0/20:4, PC 16:0/20:4 and PI 16:0/20:4), which exhibit a significant decrease of relative concentrations in tumor tissues. PE 36:4 is the most markedly down-regulated lipid in the S-plot of OPLS method. Palmitic acyl (16:0) is associated with the proliferation and arachidonic acyl (20:4) with inflammatory processes in the organism and these effects are associated with the tumor progression. Most up-regulated lipid species are PE species containing one polyunsaturated fatty acyl (22:4 and 22:5) except for PE 38:3 (18:0 and 20:3), while all down-regulated lipid species contain mainly saturated or eventually low unsaturated fatty acyls except for PE 36:4 containing arachidonic acyl. The association of saturation level with the tissue type is noticed for 10 most significantly regulated lipids.

Acknowledgments

This work was supported by ERC CZ project No. LL1302 sponsored by the Ministry of Education, Youth and Sports of the Czech Republic. E.C. acknowledges the support of the grant project No. CZ.1.07/2.3.00/30.0021 sponsored by the Ministry of Education, Youth and Sports of the Czech Republic. The help of Blanka Červená and Magdaléna Ovčačíková (University of Pardubice) with the extraction procedure is acknowledged.

Appendix A. Supplementary data

Supplementary data associated with this article can be found, in the online version, at http://dx.doi.org/10.1016/j.jchromb.2015.07.011

References

[1] D. Barh, A. Carpi, M. Verma, M. Gunduz, Cancer Biomarkers, CRC Press, Boca Raton, FL, USA, 2014.
[2] S. Pelengaris, M. Khan, The Molecular Biology of Cancer. A Bridge from Bench to Bedside, Wiley-Blackwell, Oxford, UK, 2013.
[3] W. Al-Zhoughbi, J.F. Huang, G.S. Paramasivan, H. Till, M. Pichler, B. Guertl-Lackner, G. Hoefler, Tumor macroenvironment and metabolism, Semin. Oncol. 41 (2014) 281.
[4] M.P. Wymann, R. Schneiter, Lipid signalling in disease, Nat. Rev. Mol. Cell Biol. 9 (2008) 162.
[5] L. Arana, P. Gangoiti, A. Ouro, M. Trueba, A. Gomez-Munoz, Ceramide and ceramide 1-phosphate in health and disease, Lipids Health Dis. 9 (2010) 15.
[6] G.B. Mills, W.H. Moolenaar, The emerging role of lysophosphatidic acid in cancer, Nat. Rev. Cancer 3 (2003) 582.
[7] S.M. Louie, L.S. Roberts, M.M. Mulvihill, K.X. Luo, D.K. Nomura, Cancer cells incorporate and remodel exogenous palmitate into structural and oncogenic signaling lipids, Biochim. Biophys. Acta Mol. Cell Biol. Lipids 1831 (2013) 1566.
[8] D.G. McLaren, P.L. Miller, M.E. Lassman, J.M. Castro-Perez, B.K. Hubbard, T.P. Roddy, An ultraperformance liquid chromatography method for the normal-phase separation of lipids, Anal. Biochem. 414 (2011) 266.
[9] M. Holčapek, E. Cífková, B. Červená, M. Lísa, J. Vostálová, J. Galuszka, Determination of nonpolar and polar lipid classes in human plasma, erythrocytes and plasma lipoprotein fractions using ultrahigh-performance liquid chromatography-mass spectrometry, J. Chromatogr. A 1377 (2015) 85.
[10] M. Lísa, E. Cífková, M. Holčapek, Lipidomic profiling of biological tissues using off-line two-dimensional high-performance liquid chromatography mass spectrometry, J. Chromatogr. A 1218 (2011) 5146.
[11] K. Sandra, A.D. Pereira, G. Vanhoenacker, F. David, P. Sandra, Comprehensive blood plasma lipidomics by liquid chromatography/quadrupole time-of-flight mass spectrometry, J. Chromatogr. A 1217 (2010) 4087.
[12] X.L. Han, K. Yang, R.W. Gross, Multi-dimensional mass spectrometry-based shotgun lipidomics and novel strategies for lipidomic analyses, Mass Spectrom. Rev. 31 (2012) 134.
[13] D. Schwudke, G. Liebisch, R. Herzog, G. Schmitz, A. Shevchenko, Lipidomics and Bioactive Lipids, Elsevier Academic Press Inc, San Diego, USA, 2007, pp. 175.
[14] K. Yang, H. Cheng, R.W. Gross, X.L. Han, Automated lipid identification and quantification by multidimensional mass spectrometry-based shotgun lipidomics, Anal. Chem. 81 (2009) 4356.
[15] M. Scherer, K. Leuthauser-Jaschinski, J. Ecker, G. Schmitz, G. Liebisch, A rapid and quantitative LC–MS/MS method to profile sphingolipids, J. Lipid Res. 51 (2010) 2001.
[16] E. Cífková, M. Holčapek, M. Lísa, Nontargeted lipidomic characterization of porcine organs using hydrophilic interaction liquid chromatography and off-line two-dimensional liquid chromatography-electrospray ionization mass spectrometry, Lipids 48 (2013) 915.
[17] E. Cífková, M. Holčapek, M. Lísa, M. Ovčačíková, A. Lyčka, F. Lynen, P. Sandra, Nontargeted quantitation of lipid classes using hydrophilic interaction liquid chromatography–electrospray ionization mass spectrometry with single internal standard and response factor approach, Anal. Chem. 84 (2012) 10064.
[18] J.P. Sundelin, M. Stahlman, A. Lundqvist, M. Levin, P. Parini, M.E. Johansson, J. Boren, Increased expression of the very low-density lipoprotein receptor mediates lipid accumulation in clear cell renal cell carcinoma, PLoS One 7 (2012) e48694.
[19] A.L. Dill, L.S. Eberlin, C. Zheng, A.B. Costa, D.R. Ifa, L.A. Cheng, T.A. Masterson, M.O. Koch, O. Vitek, R.G. Cooks, Multivariate statistical differentiation of renal cell carcinomas based on lipidomic analysis by ambient ionization imaging mass spectrometry, Anal. Bioanal. Chem. 398 (2010) 2969.
[20] E.E. Jones, T.W. Powers, B.A. Neely, L.H. Cazares, D.A. Troyer, A.S. Parker, R.R. Drake, MALDI imaging mass spectrometry profiling of proteins and lipids in clear cell renal cell carcinoma, Proteomics 14 (2014) 924.
[21] V. Pirro, L.S. Eberlin, P. Oliveri, R.G. Cooks, Interactive hyperspectral approach for exploring and interpreting DESI–MS images of cancerous and normal tissue sections, Analyst 137 (2012) 2374.
[22] K. Yoshimura, L.C. Chen, M.K. Mandal, T. Nakazawa, Z. Yu, T. Uchiyama, H. Hori, K. Tanabe, T. Kubota, H. Fujii, R. Katoh, K. Hiraoka, S. Takeda, Analysis of renal cell carcinoma as a first step for developing mass spectrometry-based diagnostics, J. Am. Soc. Mass Spectrom. 23 (2012) 1741.
[23] F. Sullentrop, D. Moka, S. Neubauer, G. Haupt, U. Engelmann, J. Hahn, H. Schicha, P-31 NMR spectroscopy of blood plasma: determination and quantification of phospholipid classes in patients with renal cell carcinoma, NMR Biomed. 15 (2002) 60.
[24] L. Eriksson, T. Byrne, E. Johansson, J. Trygg, C. Vikström, Multi- and Megavariate Data Analysis. Basic Principles and Applications, MKS Umetrics AB, Malmö, Sweden, 2013.
[25] G.M. Kirwan, E. Johansson, R. Kleemann, E.R. Verheij, A.M. Wheelock, S. Goto, J. Trygg, C.E. Wheelock, Building Multivariate Systems Biology Models, Anal. Chem. 84 (2012) 7064.
[26] J. Trygg, S. Wold, Orthogonal projections to latent structures (O-PLS), J. Chemom. 16 (2002) 119.
[27] S. Wold, M. Sjostrom, L. Eriksson, PLS-regression: a basic tool of chemometrics, Chemom. Intell. Lab. Syst. 58 (2001) 109.
[28] J. Folch, M. Lees, G.H.S. Stanley, A simple method for the isolation and purification of total lipides from animal tissues, J. Biol. Chem. 226 (1957) 497.
[29] E. Cífková, M. Holčapek, M. Lísa, D. Vrána, J. Gatěk, B. Melichar, Determination of lipidomic differences between human breast cancer and surrounding normal tissues using HILIC-HPLC/ESI–MS and multivariate data analysis, Anal. Bioanal. Chem. 407 (2015) 991.